COMPDYN 2011
ECCOMAS Thematic Conference on
Computational Methods in Structural Dynamics and Earthquake Engineering
M. Papadrakakis, M. Fragiadakis, V. Plevris (eds.)
Corfu, Greece, 25-28 May 2011

NON-CONFORMING SPECTRAL APPROXIMATIONS FOR THE ELASTIC WAVE EQUATION IN HETEROGENEOUS MEDIA

I. Mazzieri[1,3], C. Smerzini[2], P.F. Antonietti[1], F. Rapetti[3], M. Stupazzini[4], R. Paolucci[2] and A. Quarteroni[1,5]

[1] MOX - Modelling and Scientific Computing, Department of Mathematics, Politecnico di Milano,
P.za Leonardo da Vinci, 32, 20133 Milano, Italy.
e-mail: ilario.mazzieri@mail.polimi.it, paola.antonietti@polimi.it

[2] Department of Structural Engineering, Politecnico di Milano
P.za Leonardo da Vinci, 32, 20133 Milano, Italy.
e-mail: csmerzini@stru.polimi.it

[3] Université de Nice Sophia Antipolis, Laboratoire de Mathématiques J.A. Dieudonné,
Parc Valrose, Cedex 02, 06108 Nice, France.
frapetti@unice.fr

[4] Munich RE,
Königinstr. 107, 80802 Munich, Germany.
MStupazzini@munichre.com

[5] Chair of Modelling and Scientific Computing (CMCS),
Mathematics Institute of Computational Science and Engineering (MATHICSE),
École Polytechnique Fédérale de Lausanne (EPFL),
Station 8, 1015 Lausanne, Switzerland.
alfio.quarteroni@epfl.ch

Keywords: Computational seismology, Non-conforming approximations, Mortar Spectral Element Method, Discontinuous Galerkin Spectral Element Method.

Abstract. *Non-conforming techniques as the Mortar spectral Element Method (MSEM) or the Discontinuous Galerkin Spectral Element Method (DGSEM) are variational approaches to discretize partial differential equations, that rely on a spectral finite element approximation of a non-overlapping subdomain partition of the computational domain. In this contribution we compare and analyse MSEM and DGSEM, giving more details on the algorithmic aspects of the two non-conforming approaches, and we address their applicability and flexibility to handle seismic wave propagation problems. The numerical strategies are implemented in the spectral elements based code GeoELSE [14].*

1 INTRODUCTION

During the last three decades seismology is undergoing a major transformation at both the research and the application level. In modern seismology the classical scientific approach based on laboratory experiments has being replaced by computer simulations. Indeed, the rapid development of efficient numerical methods, gives the chance to simulate, with high resolution the complete seismic waveform field in highly heterogeneous earth media with complex geometries and up to relatively large frequencies (about 3 Hz).
The recent developments on computational seismology have been based on high-order numerical modelling of wave propagation (see, for example, [5, 12, 13, 15, 16, 17]). The reasons for using spectral element based approximations are the following. Firstly the flexibility in handling complex geometries, retaining the spatial exponential convergence for locally smooth solutions. Secondly, spectral element methods are based on the weak formulation of the elastodynamic equations involving only first-order spatial derivatives. Finally spectral element methods retain a high level parallel structure, and are therefore well suited for parallel computers.
In this paper we consider two different non-conforming high-order techniques, namely the Mortar Spectral Element Method (MSEM) and the Discontinuous Galerkin Spectral Element Method (DGSEM) to simulate seismic wave propagation in heterogeneous media. In contrast to standard conforming discretizations, as Spectral Element Method (SEM), these techniques have the further advantages that they can accommodate discontinuities, not only in the parameters, but also in the wave-field, they are energy conservative and well suited for parallel implementation. In our contribution we compare their performances when effectively applied to real problems. The paper is organized as follows. In Section 2 we recall the model problem under investigation. In Section 3 the non-conforming formulations are summarized. In Sections 4 we introduce the corresponding algebraic formulations and next, in Section 5 we describe how two efficiently implement them in a numerical code. In order to show an effective application of the methods previously described, in Section 6 a complex soil-structure interaction is studied using the MSEM and the DGSEM discretizations. Finally, in Section 7, we draw some conclusions.

2 FORMULATION OF PROBLEM

Fixing the temporal interval $(0, T]$, with $T > 0$, the equilibrium equations for an elastic medium, occupying a finite region $\Omega \subset \mathbb{R}^d$, $d = 2, 3$, subjected to an external force $\mathbf{f}$ read:

$$\rho \partial_{tt} \mathbf{u} - \nabla \cdot \underline{\sigma}(\mathbf{u}) = \mathbf{f} + \mathbf{f}^{visc}(\dot{\mathbf{u}}, \mathbf{u}), \tag{1}$$

where $\mathbf{u}$ is the displacement of the body, $\underline{\sigma}$ the stress tensor, t the time and ρ the density of the material. Since we are dealing with viscoelastic materials, we introduce in model (1) a structural damping in the form of volumetric forces $\mathbf{f}^{visc}(\dot{\mathbf{u}}, \mathbf{u}) = -2\rho\zeta\dot{\mathbf{u}} - \rho\zeta^2\mathbf{u}$, where ζ is a spatially variable (i.e., piecewise constant) suitable decay factor with dimension of inverse of the time [8]. It is worth remarking that the introduction of $\mathbf{f}^{visc}$ in (1) results in a frequency proportional quality factor, i.e. a non dispersive wave propagation (for further details see [18]).
We denote by $\Gamma = \Gamma_D \cup \Gamma_N \cup \Gamma_{NR}$ the boundary of the physical domain Ω and without loss of generality on the boundary Γ we make the following assumptions (cf [22]):

- on Γ_D the body is rigidly fixed in the space,
- on Γ_N we prescribe surface tractions ($\underline{\sigma}(\mathbf{u}) \cdot \mathbf{n} = \mathbf{t}$),
- on Γ_{NR} non-reflecting boundary conditions are imposed: cf. [27], for example.

Hereafter, an underlying bar denotes matrix or tensor quantities, while vectors are typed in bold. Moreover, we adopt the standard notation $(\cdot,\cdot)_\Omega$ to denote the L^2-inner product for scalar, vectorial and tensorial functions defined in Ω. To ease of presentation we describe the numerical methods in the case of null viscoelastic forces, i.e. $\mathbf{f}^{visc}(\dot{\mathbf{u}},\mathbf{u}) = 0$ (see Section 4.1 below for the general case).
Defining $V = \{\mathbf{v} \in [H^1(\Omega)]^d : \mathbf{v} = \mathbf{0} \text{ on } \Gamma_D\}$, the variational formulation of (1) reads:
$\forall t \in (0,T]$ *find* $\mathbf{u} = \mathbf{u}(t) \in V$ *such that*

$$\mathrm{d}_{tt}\left(\rho\mathbf{u},\mathbf{v}\right)_\Omega + \mathcal{A}(\mathbf{u},\mathbf{v})_\Omega = \mathcal{L}(\mathbf{v}), \quad \forall\,\mathbf{v} \in V, \tag{2}$$

where the bilinear form $\mathcal{A}(\cdot,\cdot) : V \times V \to \mathbb{R}^d$ is defined as $\mathcal{A}(\mathbf{u},\mathbf{v})_\Omega = (\underline{\sigma}(\mathbf{u}),\underline{\varepsilon}(\mathbf{v}))_\Omega$, and the linear functional $\mathcal{L} : V \to \mathbb{R}^d$ as $\mathcal{L}(\mathbf{v}) = (\mathbf{t},\mathbf{v})_{\Gamma_N} + (\mathbf{t}^*,\mathbf{v})_{\Gamma_{NR}} + (\mathbf{f},\mathbf{v})_\Omega$. We suppose that the strain tensor $\underline{\varepsilon}$ and the stress tensor $\underline{\sigma}$ are related through the Hooke's law

$$\underline{\varepsilon}(\mathbf{u}) = \frac{1}{2}(\nabla\mathbf{u} + \nabla\mathbf{u}^\top), \quad \underline{\sigma}(\mathbf{u}) = \lambda\nabla\cdot\mathbf{u}\,\underline{\mathrm{I}} + 2\mu\underline{\varepsilon}(\mathbf{u}),$$

where $\underline{\mathrm{I}}$ is the $d-$dimensional identity tensor and λ and μ are the Lamé elastic coefficients. We remark that for heterogeneous media ρ,λ and μ are bounded functions of the spatial variable, not necessarily continuous i.e., ρ,λ and $\mu \in L^\infty(\Omega)$. Finally, to complete problem (2), we prescribe initial conditions $\mathbf{u}_0$ and $\mathbf{u}_1$ for the displacement and the velocity, respectively.
It can be proved that the bilinear form $\mathcal{A}(\cdot,\cdot)$ is symmetric, V-elliptic and continuous. These conditions imply that problem (2) admits a unique solution, (cf. [4, 23]).
Let V_δ be a suitable finite dimensional approximation of the space V, the semi-discrete approximation of (2) reads : $\forall t \in (0,T]$ *find* $\mathbf{u}_\delta = \mathbf{u}_\delta(t) \in V_\delta$ *such that*

$$\mathrm{d}_{tt}\left(\rho\mathbf{u}_\delta,\mathbf{v}\right)_\Omega + \mathcal{A}(\mathbf{u}_\delta,\mathbf{v}) = \mathcal{L}(\mathbf{v}), \quad \forall\,\mathbf{v} \in V_\delta. \tag{3}$$

In general, in non-conforming approximations, the space V_δ is not a subspace of V. In the following section we describe how to build V_δ for both for the Mortar Spectral Element Method (MSEM) and the Discontinuous Galerkin Spectral Element Method (DGSEM).

3 NON CONFORMING FORMULATIONS

To approximate the problem (3) we start by a discretization of the spatial differential operators in Ω, that rely on a time-independent three-level spatial decomposition of the domain Ω.
At the first level, we subdivide Ω into K non overlapping regions Ω_k, $k = 1,...,K$, such that $\overline{\Omega} = \bigcup_{k=1}^K \overline{\Omega}_k$ with $\Omega_k \cap \Omega_\ell = \emptyset$ if $k \neq \ell$ and we define the skeleton of this (macro) decomposition as $\mathcal{S} = \bigcup_{k=1}^K \partial\Omega_k \backslash \partial\Omega$. Note that this decomposition can be geometrically non-conforming, i.e., for two neighbouring subdomains Ω_k, Ω_ℓ, the interface $\gamma = \partial\Omega_k \cap \partial\Omega_\ell$ may not be a complete side (for $d = 2$) or face (for $d = 3$) of Ω_k or Ω_ℓ.
To get the second level, in each Ω_k we introduce a (meso) partitioning $\mathcal{T}_{h_k}$, made by elements Ω_k^j that are image through an invertible mapping F_k^j of the reference element $\hat{\Omega} = (-1,1)^d$. The quadrilaterals Ω_k^j, if $d = 2$, or hexahedra, if $d = 3$, have typical linear size h_k and $\overline{\Omega}_k = \bigcup_{j=1}^{J_k} \overline{\Omega}_k^j$.
The third (micro) level is represented by the so-called Gauss-Lobatto-Legendre (GLL) points in each mesh element Ω_k^j. Let $\hat{\mathbf{Q}}_{N_k}(\hat{\Omega})$ be the space of functions defined on $\hat{\Omega}$ that are algebraic polynomials of degree less than or equal to $N_k \geq 2$ in each spatial variable $x_1,...,x_d$. Thus, we set

$$\mathbf{Q}_{N_k}(\Omega_k^j) = \left\{ v = \widehat{v} \circ {F_k^j}^{-1} : \widehat{v} \in \hat{\mathbf{Q}}_{N_k}(\hat{\Omega}) \right\},$$

and we define the finite dimensional space $X_\delta(\Omega_k)$ as

$$X_\delta(\Omega_k) = \left\{ v_\delta \in \mathcal{C}^0(\overline{\Omega}_k) : v_{\delta|\Omega_k^j} \in \mathbf{Q}_{N_k}(\Omega_k^j)\ \forall \Omega_k^j \in \mathcal{T}_{h_k} \right\},$$

and finally $V_\delta = \{\mathbf{v}_\delta \in [L^2(\Omega)]^d : \mathbf{v}_{\delta|\Omega_k} \in [X_\delta(\Omega_k)]^d\ \ \forall k = 1, ..., K : \mathbf{v}_{\delta|\Gamma_D} = \mathbf{0}\}$. Here $\delta = \{\mathbf{h}, \mathbf{N}\}$ with $\mathbf{h} = (h_1, ..., h_K)$ and $\mathbf{N} = (N_1, ..., N_K)$ are K-uplets of discretization parameters. Problem (3) is then equivalent to: $\forall t \in (0, T]$ *find* $(\mathbf{u}_{\delta,1}(t), \ldots, \mathbf{u}_{\delta,K}(t)) \in V_\delta$ *such that*

$$\sum_{k=1}^{K} \mathrm{d}_{tt}(\rho \mathbf{u}_{\delta,k}, \mathbf{v}_k)_{\Omega_k} + \mathcal{A}(\mathbf{u}_{\delta,k}, \mathbf{v}_k)_{\Omega_k} + \mathcal{B}(\mathbf{u}_{\delta,k}, \mathbf{v}_k)_{\partial\Omega_k \setminus \partial\Omega} = \sum_{k=1}^{K} \mathcal{L}(\mathbf{v}_k)_{\Omega_k}, \tag{4}$$

for all $(\mathbf{v}_1, \ldots, \mathbf{v}_K) \in V_\delta$, where

$$\mathcal{A}(\mathbf{u}, \mathbf{v})_{\Omega_k} = (\underline{\sigma}(\mathbf{u}), \underline{\varepsilon}(\mathbf{v}))_{\Omega_k}, \quad \text{and} \quad \mathcal{B}(\mathbf{u}, \mathbf{v})_{\partial\Omega_k \setminus \partial\Omega} = (\underline{\sigma}(\mathbf{u}) \cdot \mathbf{n}, \mathbf{v})_{\partial\Omega_k \setminus \partial\Omega}. \tag{5}$$

Depending on the chosen non-conforming approach, the functional space V_δ is completed by additional conditions on $\mathbf{u}_{\delta,k}$, $k = 1, \ldots, K$, on the skeleton of the macro decomposition which ensure that $\mathbf{u}_{\delta,k}$ is the restriction to Ω_k of $\mathbf{u}_\delta \in H^1(\Omega)^d$. The bilinear form $\mathcal{B}(\cdot, \cdot)$ may either be zero or gather all the contributions $(\sigma(\mathbf{u}_{\delta,k}) \cdot \mathbf{n}_k, \mathbf{v}_k)_{\partial\Omega_k \setminus \partial\Omega}$, $k = 1, \ldots, K$, depending on the chosen approach. Equation (4) represents the starting point to introduce the MSEM and the DGSEM.
In the next sections we describe the two approaches. To ease the presentation, we suppose that $\Gamma_D = \partial\Omega$ and we assume that each partition $\mathcal{T}_{h_k}$ of Ω_k consists in only one element, i.e., Ω is subdivided into K non-overlapping spectral elements $\Omega_1, ..., \Omega_K$ so that $\overline{\mathcal{S}} = \bigcap_{k=1}^{K} \partial\overline{\Omega}_k \setminus \Gamma_D$. The more general case follows from similar arguments.

3.1 Mortar Spectral Formulation

In this section we introduce the MSEM for the solution of (4), see [11, 21] for a more detailed description. We denote by Γ_k^ℓ, $\ell = 1, \ldots, 2d$, the edges (faces) of each subdomain Ω_k, $k = 1, \ldots, K$, so that $\partial\Omega_k = \bigcup_{\ell=1}^{2d} \overline{\Gamma}_k^\ell$. We then identify the skeleton $\mathcal{S}$ as the union of elementary non-empty components called *mortars* (or *masters*), more precisely

$$\mathcal{S} = \bigcup_{k=1}^{K} (\partial\Omega_k \setminus \partial\Omega) = \bigcup_{m=1}^{M} \overline{\gamma}_m, \quad \text{with } \gamma_m \cap \gamma_n = \emptyset, \quad \text{if } m \neq n, \tag{6}$$

where each mortar is a whole edge (or face) $\Gamma_{k(m)}^{\ell(m)}$ of a specific element $\Omega_{k(m)}$ and m is an arbitrary numbering $m = 1, \ldots, M$, with M a positive integer. Those edges or faces Γ_k^ℓ that do not coincide with a mortar are called *non-mortars* (or *slaves*) and provide a dual description of the skeleton, as

$$\mathcal{S} = \bigcup_{m\, mortar} \gamma_m^+ = \bigcup_{n\, non\, mortar} \gamma_n^-.$$

The intersection of the closures of the mortars defines a set of vertices or *cross-points*

$$\mathcal{V} = \{\mathbf{x}_q = (\overline{\gamma}_r^+ \cap \overline{\gamma}_s^+),\ \mathbf{x}_q \notin \overline{\gamma}_m^+,\ m = 1, \ldots, M\},$$

where q is an arbitrary numbering $q = 1, \ldots, \mathtt{V}$. We define as well the set $\widetilde{\mathcal{V}}$ of *virtual* vertices (that are not cross-points) as $\widetilde{\mathcal{V}} = \{\widetilde{\mathbf{x}}_q = (\overline{\gamma}_r^+ \cap \gamma_s^+)\}$, where q is an arbitrary numbering

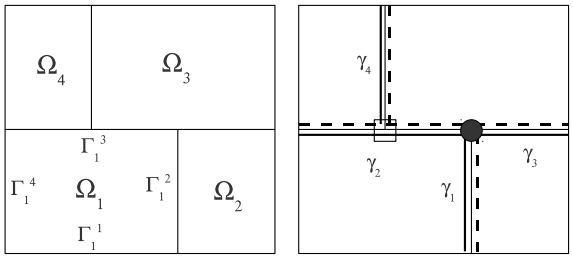

Figure 1: Nonconforming domain decomposition (left) and skeleton structure (right) showing a cross-point (•), a virtual vertex (□), the mortars (dark continuous lines) and the non-mortars (dark dashed lines).

$q = 1, \ldots, \widetilde{\mathrm{V}}$ (see Fig. 1). Let $\Lambda_\delta(\Gamma_k^\ell) = \mathbf{Q}_{N_k}(\Gamma_k^\ell)$ be the space of the traces of functions of $X_\delta(\Omega_k)$ over Γ_k^ℓ and $\widehat{\Lambda}_\delta(\Gamma_k^\ell) = \mathbf{Q}_{N_k-2}(\Gamma_k^\ell)$. We can now define the nonconforming spectral element discretization space $\widetilde{V}_\delta$ as the space of functions $\mathbf{v}_\delta \in V_\delta$ that satisfy the following additional *mortar matching condition*:

(MC) let $\mathbf{\Phi}$ be the *mortar function* associated with $\mathbf{v}_\delta$, i.e., a function that is continuous on $\mathcal{S}$, zero on $\partial\Omega$ and such that on each mortar $\gamma_m = \Gamma_{k(m)}^{\ell(m)}$ coincides with the restriction of $\mathbf{v}_{\delta,k} = \mathbf{v}_{\delta|\Omega_k}$ to γ_m; then, for all indices (k,ℓ) such that Γ_k^ℓ is contained in $\mathcal{S}$ but $(k,\ell) \neq (k(m),\ell(m))$ for all $m = 1,\ldots,M$ (that is for all indices (k,ℓ) such that Γ_k^ℓ is a *non-mortar*) we require that:

$$\int_{\Gamma_k^\ell} (\mathbf{v}_{\delta,k} - \mathbf{\Phi}) \cdot \hat{\mathbf{\Phi}}\, d\gamma = 0 \quad \forall \hat{\mathbf{\Phi}} \in [\widehat{\Lambda}_\delta(\Gamma_k^\ell)]^d, \tag{7}$$

and that

$$\mathbf{v}_{\delta|\Omega_k}(\mathbf{x}_q) = \mathbf{\Phi}(\mathbf{x}_q), \quad \forall\, \mathbf{x}_q \in \mathcal{V} \cup \widetilde{\mathcal{V}}. \tag{8}$$

The integral matching condition (7) represents a minimization of the jump in functions at internal boundaries with respect to the L^2 norm. The vertex condition (8) ensures exact continuity at cross-points.

The Mortar Spectral Formulation is obtained by solving in each region Ω_k the elastodynamic variational problem (4) with homogeneous Neumann boundary conditions on $\mathcal{S}$ ($\underline{\sigma}(\mathbf{u}) \cdot \mathbf{n} = \mathbf{0}$ so that $\sum_k \mathcal{B}(\mathbf{u},\mathbf{v})_{\partial\Omega_k \setminus \partial\Omega}$ is identically zero), and enforcing weak continuity of the displacement on $\mathcal{S}$ with *mortar condition* (7). Thus, the semi-discrete Mortar Spectral Formulation reads:

$\forall t \in (0,T]$ *find* $(\mathbf{u}_{\delta,1}(t), \ldots, \mathbf{u}_{\delta,K}(t)) \in V_\delta^{mortar}$ *such that*

$$\sum_k d_{tt}\left(\rho \mathbf{u}_{\delta,k}, \mathbf{v}_k\right)_{\Omega_k} + \mathcal{A}(\mathbf{u}_{\delta,k}, \mathbf{v}_k)_{\Omega_k} = \sum_k \mathcal{L}(\mathbf{v}_k), \quad \forall\, (\mathbf{v}_1, \ldots, \mathbf{v}_K) \in V_\delta^{mortar}, \tag{9}$$

where $V_\delta^{mortar} = \{(\mathbf{v}_1, \ldots, \mathbf{v}_K) \in V_\delta$: the $mortar\ condition$ **(MC)** is satisfied$\}$.

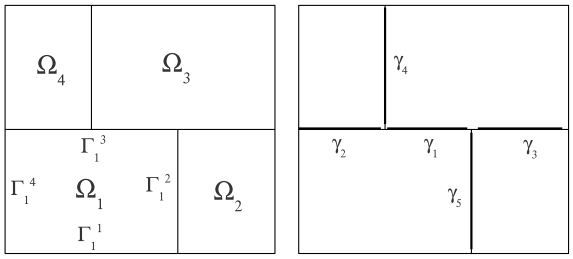

Figure 2: Nonconforming domain decomposition (left) and skeleton structure (right) showing the elementary components (dark continuous lines).

3.2 Discontinuous Galerkin Spectral Formulation

In order to introduce the Discontinuous Galerkin Spectral Formulations, we subdivide the skeleton $\mathcal{S}$ in the set of elementary components (edges if $d = 2$, faces if $d = 3$) as follows:

$$\overline{\mathcal{S}} = \bigcup_{j=1}^{M} \overline{\gamma}_j, \quad \text{with } \gamma_i \cap \gamma_j = \emptyset, \quad \text{if } i \neq j, \tag{10}$$

where each edge (face) is given by $\overline{\gamma}_j = (\partial\overline{\Omega}_{k(j)} \cap \partial\overline{\Omega}_{\ell(j)}) \setminus \partial\Omega$, for some different positive integers k and ℓ. Notice that this decomposition is unique (see Fig. 2). Next, we collect all the edges (faces) in the set $\mathcal{F}_I$. For regular enough functions, we use the standard notation [2] to define the jumps ($[\![\cdot]\!]$) and the average ($\{\cdot\}$) operators on each edge (face) $\gamma \in \mathcal{F}_I$.
We obtain the following semi-discrete DG Spectral Formulation:
$\forall t \in (0, T]$ *find* $\mathbf{u}_\delta = (\mathbf{u}_{\delta,1}(t), ..., \mathbf{u}_{\delta,K}(t)) \in V_\delta^{DG} \equiv V_\delta$ *such that*

$$\sum_{k=1}^{K} \left(\mathrm{d}_{tt} \left(\rho \mathbf{u}_\delta, \mathbf{v} \right)_{\Omega_k} + \mathcal{A}(\mathbf{u}_\delta, \mathbf{v})_{\Omega_k} \right) + \sum_{j=1}^{M} \mathcal{B}(\mathbf{u}_\delta, \mathbf{v})_{\gamma_j} = \mathcal{L}(\mathbf{v}) \quad \forall\, \mathbf{v} = (\mathbf{v}_1, ..., \mathbf{v}_K) \in V_\delta^{DG}, \tag{11}$$

with

$$\mathcal{B}(\mathbf{u}_\delta, \mathbf{v})_{\gamma_j} = -\left(\{\underline{\sigma}(\mathbf{u}_\delta)\}, [\![\mathbf{v}]\!] \right)_{\gamma_j} + \theta \left([\![\mathbf{u}_\delta]\!], \{\underline{\sigma}(\mathbf{v})\} \right)_{\gamma_j} + \eta_{\gamma_j} \left([\![\mathbf{u}_\delta]\!], [\![\mathbf{v}]\!] \right)_{\gamma_j}. \tag{12}$$

Here $\eta_{\gamma_j} = \frac{\alpha \mathtt{N}_\mathtt{j}^2}{\mathtt{h}_\mathtt{j}} \{\lambda + 2\mu\}_A$, where $\{\cdot\}_A$ represents the harmonic average, $\mathtt{N}_\mathtt{j} = \max(N_{k(j)}, N_{\ell(j)})$, $\mathtt{h}_\mathtt{j} = \min(h_{k(j)}, h_{\ell(j)})$ and α is a positive constant at our disposal. Corresponding to different values of θ we obtain different DG schemes, namely: $\theta = -1$ (resp. $\theta = 1$) leads to the symmetric (resp. non-symmetric) interior penalty method, while $\theta = 0$ corresponds to the so-called incomplete interior penalty method (see [2, 24, 25, 26] for more details).

4 ALGEBRAIC FORMULATION AND TIME INTEGRATION SCHEME

We discuss here the algebraic formulation of the two non-conforming approaches presented in the previous section. In particular we described how to build the linear systems coming from the mortar or DG discretization and discuss the time integration scheme.

4.1 Algebraic formulation of the problem

We denote by $D = \sum_{k=1}^{K}(N_k+1)^2$ the dimension of each component of V_δ and we introduce a basis $\{\mathbf{\Psi}_i^1, \mathbf{\Psi}_i^2\}_{i=1}^D$ for the finite dimensional space V_δ, where $\mathbf{\Psi}_i^1 = (\Psi_i^1, 0)^\top$ and $\mathbf{\Psi}_i^2 = (0, \Psi_i^2)^\top$. We choose the set of shape functions in such a way that they are orthonormal with respect to the L^2 inner product on the reference element.
We denote by $\{\mathbf{p}_j\}_{j=1}^D$ the GLL nodes of the mesh and we suppose that $\Psi_i^1(\mathbf{p}_j) = \Psi_i^2(\mathbf{p}_j) = \delta_{ij}$, for $i, j = 1, ..., D$, where δ_{ij} represents the Kronecker symbol. Dropping the subscript δ, we write the trial functions $\mathbf{u} \in V_\delta$ as a linear combination of the basis functions

$$\mathbf{u}(\mathbf{x}, t) = \sum_{j=1}^{D} \begin{bmatrix} \Psi_j^1(\mathbf{x}) \\ 0 \end{bmatrix} U_j^1(t) + \sum_{j=1}^{D} \begin{bmatrix} 0 \\ \Psi_j^2(\mathbf{x}) \end{bmatrix} U_j^2(t).$$

Next, we define $a_k = 1 + \sum_{j=1}^{k-1}(N_j+1)^2$ and $b_k = \sum_{j=1}^{k}(N_j+1)^2$ and we order the basis functions such that

$$\mathbf{u}_{|\Omega_k} = \left(u^1, u^2\right)^\top_{|\Omega_k} = \left(\sum_{j=a_k}^{b_k} \Psi_j^1 U_{j,k}^1 \,, \sum_{j=a_k}^{b_k} \Psi_j^2 U_{j,k}^2 \right)^\top, \quad \text{for } k = 1, ..., K.$$

With such a notation (11) can be rewritten as the following set of ODE

$$\begin{bmatrix} \underline{\mathrm{M}}^1 & \underline{0} \\ \underline{0} & \underline{\mathrm{M}}^2 \end{bmatrix} \begin{bmatrix} \ddot{\mathbf{U}}^1 \\ \ddot{\mathbf{U}}^2 \end{bmatrix} + \begin{bmatrix} \underline{\mathrm{A}}^1 + \underline{\mathrm{B}}^1 & \underline{\mathrm{A}}^2 + \underline{\mathrm{B}}^2 \\ \underline{\mathrm{A}}^3 + \underline{\mathrm{B}}^3 & \underline{\mathrm{A}}^4 + \underline{\mathrm{B}}^4 \end{bmatrix} \begin{bmatrix} \mathbf{U}^1 \\ \mathbf{U}^2 \end{bmatrix} = \begin{bmatrix} \mathbf{F}^{ext,1} \\ \mathbf{F}^{ext,2} \end{bmatrix}, \tag{13}$$

where $\ddot{\mathbf{U}}$ represents the vector of the nodal acceleration and $\mathbf{F}^{ext}$ the vector of externally applied loads. As a consequence of our assumptions on the basis functions, the mass matrices $\underline{\mathrm{M}}^1$ and $\underline{\mathrm{M}}^2$ have a block diagonal structure, i.e., $\underline{\mathrm{M}}^\ell = \mathtt{diag}(\underline{\mathrm{M}}_1^\ell, \underline{\mathrm{M}}_2^\ell, ..., \underline{\mathrm{M}}_K^\ell)$, for $\ell = 1, 2$, where each block $\underline{\mathrm{M}}_k^\ell$ is associated to the spectral element Ω_k and $\mathrm{M}_k^\ell(i,j) = (\rho\Psi_j^\ell, \Psi_i^\ell)_{\Omega_k}$, for $i, j = a_k, ..., b_k$. The matrix $\underline{\mathrm{A}}$ associated to the bilinear form $\mathcal{A}(\cdot,\cdot)$ defined in (5) takes the form

$$\underline{\mathrm{A}} = \begin{bmatrix} \underline{\mathrm{A}}^1 & \underline{\mathrm{A}}^2 \\ \underline{\mathrm{A}}^3 & \underline{\mathrm{A}}^4 \end{bmatrix},$$

where the block diagonal matrices $\underline{\mathrm{A}}^\ell$, $\ell = 1, .., 4$ are equal to $\underline{\mathrm{A}}^\ell = \mathtt{diag}(\underline{\mathrm{A}}_1^\ell, \underline{\mathrm{A}}_2^\ell, ..., \underline{\mathrm{A}}_K^\ell)$. The elements of the matrices $\underline{\mathrm{A}}_k^\ell$, $\ell = 1, ..., 4$ and $k = 1, .., K$, are defined by

$$\mathrm{A}_k^1(i,j) = \mathcal{A}(\underline{\sigma}(\mathbf{\Psi}_j^1), \underline{\varepsilon}(\mathbf{\Psi}_i^1))_{\Omega_k}, \quad \mathrm{A}_k^2(i,j) = \mathcal{A}(\underline{\sigma}(\mathbf{\Psi}_j^2), \underline{\varepsilon}(\mathbf{\Psi}_i^1))_{\Omega_k}, \text{ for } i, j = a_k, ..., b_k,$$

$$\mathrm{A}_k^3(i,j) = \mathcal{A}(\underline{\sigma}(\mathbf{\Psi}_j^1), \underline{\varepsilon}(\mathbf{\Psi}_i^2))_{\Omega_k}, \quad \mathrm{A}_k^4(i,j) = \mathcal{A}(\underline{\sigma}(\mathbf{\Psi}_j^2), \underline{\varepsilon}(\mathbf{\Psi}_i^2))_{\Omega_k}, \text{ for } i, j = a_k, ..., b_k.$$

We remark that the matrices $\underline{\mathrm{M}}$ and $\underline{\mathrm{A}}$ are very similar to those coming from the discretization of the elastodynamic equation (2) with the conforming Spectral Element Method (see [6, 7]).
If we are using the mortar formulation, the matrix $\underline{\mathrm{B}}$, associated to the bilinear form $\mathcal{B}(\cdot,\cdot)$ defined in (5), is the null matrix, whereas in the DG approach, is the one that takes into account of the discontinuity of the numerical solution across the skeleton $\mathcal{S}$. More precisely,

$$\underline{\mathrm{B}} = \begin{bmatrix} \underline{\mathrm{B}}^1 & \underline{\mathrm{B}}^2 \\ \underline{\mathrm{B}}^3 & \underline{\mathrm{B}}^4 \end{bmatrix}, \tag{14}$$

where

$$\underline{\mathrm{B}}^{\ell} = \begin{bmatrix} \underline{\mathrm{B}}^{\ell}_{1,1} & \cdots & \underline{\mathrm{B}}^{\ell}_{1,K} \\ \vdots & \ddots & \vdots \\ \underline{\mathrm{B}}^{\ell}_{K,1} & \cdots & \underline{\mathrm{B}}^{\ell}_{K,K} \end{bmatrix}, \quad \text{for } \ell = 1, ..., 4.$$

In particular the elements of each block $\underline{B}^{1}_{k,n}(i,j) = \sum_{\gamma \in \mathcal{F}_I} \mathcal{B}(\mathbf{\Psi}^1_j, \mathbf{\Psi}^1_i)_{\gamma}$, $i = a_k, ..., b_k$ and $j = a_n, ..., b_n$. The elements of the matrices $\underline{\mathrm{B}}^{\ell}_{k,n}$, for $\ell = 2, 3, 4$ are defined in a similar way.
The situation is a little bit more complicated in the Mortar approach, since the weak continuity condition across the skeleton $\mathcal{S}$ does not appear explicitly in the variational equation but it is a constraint in the functional space V^{mortar}_{δ}.
To take into account the **(MC)** we have to modify the system (13) as follows. Without loss of generality let us suppose that γ^-_n is a non mortar edge contained in $\mathcal{S}$ and that it is shared by two regions Ω_m and Ω_n. We call *master* the side of γ^-_n belonging to $\overline{\Omega}_m$ and *slave* the other side. Thus, the *mortar conditions* can be recast as:

(i) $\mathbf{\Phi} = \mathbf{u}_m$ on γ^-_n,

(ii) $\int_{\gamma^-_n} (\mathbf{u}_n - \mathbf{u}_m) \cdot \hat{\mathbf{\Phi}} ds = 0 \quad \forall \hat{\mathbf{\Phi}} \in [\widehat{\Lambda}_{\delta}(\gamma^-_n)]^d$.

At the algebraic level, the condition in $(\mathbf{ii})$ is represented by the following linear system of equations

$$\begin{bmatrix} \underline{R}^1 & \underline{0} \\ \underline{0} & \underline{R}^2 \end{bmatrix} \begin{bmatrix} \mathbf{U}^1_n \\ \mathbf{U}^2_n \end{bmatrix} = \begin{bmatrix} \underline{P}^1 & \underline{0} \\ \underline{0} & \underline{P}^2 \end{bmatrix} \begin{bmatrix} \mathbf{U}^1_m \\ \mathbf{U}^2_m \end{bmatrix}, \tag{15}$$

where

$$\underline{R}^{\ell}(i,j) = \int_{\gamma^-_n} \Psi^{\ell}_j \hat{\Phi}^{\ell}_i ds \quad \text{and} \quad \underline{P}^{\ell}(i,j) = \int_{\gamma^-_n} \Phi^{\ell}_j \hat{\Phi}^{\ell}_i ds, \quad \ell = 1, 2. \tag{16}$$

By using that the shape functions are orthonormal on the reference element and suitable quadrature rules to integrate (16), (cf. [3, 11]), it is possible to easily invert the matrix $\underline{R}$ and to reduce (15) to

$$\begin{bmatrix} \mathbf{U}^1_n \\ \mathbf{U}^2_n \end{bmatrix} = \begin{bmatrix} \underline{Q}_n & \underline{0} \\ \underline{0} & \underline{Q}_n \end{bmatrix} \begin{bmatrix} \mathbf{U}^1_m \\ \mathbf{U}^2_m \end{bmatrix},$$

where $\underline{Q}_n = (\underline{R}^1)^{-1}\underline{P}^1 = (\underline{R}^2)^{-1}\underline{P}^2$. To obtain a global projection operator $\widetilde{\underline{\mathrm{Q}}}$ we proceed as follows. For each component of $\mathbf{u}$ we denote by $\mathbf{U}_{slave}$ the vector of unknowns associated to the dofs that lay on the slave side of $\mathcal{S}$ and by $\mathbf{U}_{master}$ the vector of unknowns associated to all the remaining dofs. Then, for each γ^-_n contained into the skeleton $\mathcal{S}$ we build the local projection operator $\underline{Q}_n$ and we store it into the matrix $\widetilde{\underline{Q}}$. In this way $\widetilde{\underline{Q}}$ has a block structure of the form

$$\widetilde{\underline{\mathrm{Q}}} = \begin{bmatrix} \underline{\hat{Q}} & \underline{0} \\ \underline{0} & \underline{\hat{Q}} \end{bmatrix}, \tag{17}$$

where $\underline{\hat{Q}}$ is block diagonal matrix with a block equal to the identity and the other equal to the rectangular matrix $\underline{Q}$ containing all the local matrices $\underline{Q}_n$. Thus, we have that the global linear system can be expressed as

$$\widetilde{\underline{\mathrm{Q}}}^{\top} \widetilde{\underline{\mathrm{M}}} \widetilde{\underline{\mathrm{Q}}} \ddot{\mathbf{U}}_{master} + \widetilde{\underline{\mathrm{Q}}}^{\top} \widetilde{\underline{\mathrm{A}}} \widetilde{\underline{\mathrm{Q}}} \mathbf{U}_{master} = \widetilde{\underline{\mathrm{Q}}}^{\top} \mathbf{F}^{ext}, \tag{18}$$

where the rows and the columns of the matrices $\widetilde{\underline{\mathrm{M}}}$ and $\widetilde{\underline{\mathrm{A}}}$ have been modified according to these latter assumptions on the unknown renumbering. We remark that it is possible to obtain

the linear system (18) using as a basis for V_δ^{mortar}, the functions $\{\widetilde{\mathbf{\Psi}}_i^1, \widetilde{\mathbf{\Psi}}_i^2\}_{i=1}^D$, where $\widetilde{\mathbf{\Psi}}_i^1 = (\widetilde{\Psi}_i^1, 0)^\top$ and $\widetilde{\mathbf{\Psi}}_i^2 = (0, \widetilde{\Psi}_i^2)^\top$ are defined by

$$\widetilde{\Psi}_i^\ell = \begin{cases} \Psi_i^\ell & \forall i \text{ s.t } \mathbf{p}_i \text{ is a } \textit{master} \text{ node}, \\ \sum_j \underline{\hat{Q}}_{ij} \Psi_j^\ell & \forall i \text{ s.t } \mathbf{p}_i \text{ is a } \textit{slave} \text{ node}, (\mathbf{p}_j \textit{ master} \text{ node on } \mathcal{S}). \end{cases}$$

All the terms appearing in the algebraic formulations presented so fare are computed using the Gauss-Lobatto quadrature rule in which the quadrature points coincide with GLL points. We notice that since the term $\Psi_j \Psi_i \in \mathbf{Q}_{2N_k}$, for some k, the spectral mass matrix is slightly under integrated. However, since the Gauss-Lobatto rule with N_k points is exact for polynomials up to degree $2N_k - 1$, the final accuracy of spectral methods is not damaged [6].
Finally, we point out that if $\mathbf{f}^{visc} \neq 0$ we must compute the following additional external forces:

$$\begin{bmatrix} \mathbf{F}^{visc,1} \\ \mathbf{F}^{visc,2} \end{bmatrix} = - \begin{bmatrix} \underline{\mathrm{C}}^1 & \underline{0} \\ \underline{0} & \underline{\mathrm{C}}^2 \end{bmatrix} \begin{bmatrix} \dot{\mathbf{U}}^1 \\ \dot{\mathbf{U}}^2 \end{bmatrix} - \begin{bmatrix} \underline{\mathrm{D}}^1 & \underline{0} \\ \underline{0} & \underline{\mathrm{D}}^2 \end{bmatrix} \begin{bmatrix} \mathbf{U}^1 \\ \mathbf{U}^2 \end{bmatrix},$$

where the matrices $\underline{\mathrm{C}}^\ell$ and $\underline{\mathrm{D}}^\ell$, for $\ell = 1, 2$ have a block diagonal structure. Each block $\underline{\mathrm{C}}_k^\ell$ and $\underline{\mathrm{D}}_k^\ell$ is associated to the spectral element Ω_k and

$$\mathrm{C}_k^\ell(i,j) = (\rho\zeta\Psi_j^\ell, \Psi_i^\ell)_{\Omega_k}, \quad \mathrm{D}_k^\ell(i,j) = (\rho\zeta^2\Psi_j^\ell, \Psi_i^\ell)_{\Omega_k}, \quad \text{for } i,j = a_k, ..., b_k,$$

respectively. Then the discretized system becomes:

$$\underline{\mathrm{M}}\ddot{\mathbf{U}} + \underline{\mathrm{C}}\dot{\mathbf{U}} + (\underline{\mathrm{A}} + \underline{\mathrm{B}} + \underline{\mathrm{D}})\mathbf{U} = \mathbf{F}^{ext}, \tag{19}$$

where the accelerations $\ddot{\mathbf{U}}$ and the velocities $\dot{\mathbf{U}}$ are approximated as described in the next section.

4.2 Time integration

Let now subdivide into N subinterval of amplitude $\Delta t = \frac{T}{N}$ the interval $(0, T]$: the time integration scheme for (13) is achieved with the second order central difference scheme, setting $t_n = n\Delta t$:

$$\ddot{\mathbf{U}}(t_n) = \frac{\mathbf{U}(t_{n+1}) - 2\mathbf{U}(t_n) + \mathbf{U}(t_{n-1})}{\Delta t^2}, \quad \dot{\mathbf{U}}(t_n) = \frac{\mathbf{U}(t_{n+1}) - \mathbf{U}(t_{n-1})}{2\Delta t}. \tag{20}$$

Thus, the equation (13) or (18) at each time step t_n becomes:

$$\underline{\mathrm{K}}\mathbf{U}(t_{n+1}) = \mathbf{b}(\mathbf{U}(t_n), \mathbf{U}(t_{n-1}), \mathbf{F}^{ext}(t_n), \underline{\mathrm{A}}, \underline{\mathrm{B}}), \tag{21}$$

with initial condition $\mathbf{U}(t_0) = \mathbf{u}_0$ and $\dot{\mathbf{U}}(t_0) = \mathbf{u}_1$. If we adopt a fully explicit time integration scheme the matrix $\underline{\mathrm{K}}$ is the mass matrix, i.e. $\underline{\mathrm{K}} = \underline{\mathrm{M}}$, if a DGSEM is employed and $\underline{\mathrm{K}} = \underline{\widetilde{\mathrm{Q}}}^\top \underline{\widetilde{\mathrm{M}}}\, \underline{\widetilde{\mathrm{Q}}}$ for the MSEM. In particular, for the latter approach, taking advantage of the structure of $\underline{\widetilde{\mathrm{Q}}}$ it is possible to decompose the linear system (21) as follows

$$\begin{bmatrix} \underline{\mathrm{M}}_{master} & 0 \\ 0 & \underline{Q}^\top \underline{\mathrm{M}}_{slave} \underline{Q} \end{bmatrix} \begin{bmatrix} \mathbf{U}_{master}^{\mathcal{I}} \\ \mathbf{U}_{master}^{\mathcal{S}} \end{bmatrix} = \begin{bmatrix} \mathbf{b}_{master}^{\mathcal{I}} \\ \underline{Q}^\top \mathbf{b}_{slave}^{\mathcal{S}} \end{bmatrix}. \tag{22}$$

Here the superscripts $\mathcal{I}$ and $\mathcal{S}$ denote if the unknowns belong to the interior or to the skeleton of the domain. Then at each time step we solve separately the two blocks of the linear systems (22).

In particular for the non diagonal block we perform the LU-factorization with pivoting (cf [22]). To ensure stability, the explicit time integration scheme must satisfy the usual Courant-Friedrichs-Levy (CFL) condition (see [22]) that imposes a restriction on the amplitude of Δt. This limitation is proportional to the minimal distance Δx between two consecutive spectral nodes $\mathbf{p}_i$ and $\mathbf{p}_j$, with $i \neq j$, of the numerical grid, see [8]. Since GLL points are clustered near the edges of spectral elements Ω_k, where the grid size is proportional to N_k^{-2}, the stability requirement on Δt may become too restrictive for very large approximation orders N_k. In such cases an implicit time scheme is recommended.

5 HOW IMPLEMENTING THE METHODS

In this section we describe the implementation of the MSEM and the DGSEM in the spectral element code GeoELSE [14] and we compare the two different algorithms from the efficiency view point. In this context the word "efficiency" has the meaning of low memory storage and executing program velocity. In this sense, the assembling of the matrices in (13)-(18) is performed once, outside the time loop.
After setting the initial condition $\mathbf{u}_0$ and $\mathbf{u}_1$, we build the skeleton $\mathcal{S}$ as explained in (6)-(10) for the MSEM or the DGSEM respectively. In the mortar solution scheme, see Algorithm 1, a further step is required in order to identify the *master* and the *slave* decomposition of $\mathcal{S}$.
For both algorithms we notice that in general, all the matrix-vector multiplications involving $\underline{\mathrm{M}}, \underline{\mathrm{A}}, \underline{\mathrm{B}}$ and $\underline{Q}$ have to be intended subdomains per subdomains.

Algorithm 1: Mortar Solution Scheme

1. Set initial conditions $\mathbf{u}_0$ and $\mathbf{u}_1$.
2. Build the skeleton $\mathcal{S}$ for the domain Ω.
3. Decompose $\mathcal{S}$ into the union of *master* and *slave* edges.
4. Construct the projection operator $\underline{Q}$ for the interface unknowns $\mathbf{U}_{slave}$.
5. Perform the LU-factorization of $\underline{Q}^{\top}\underline{\mathrm{M}}_{slave}\underline{Q}$.
6. For each discrete time t_n:
   - compute the internal forces $\mathbf{F}^{int}(t_n) = \underline{\mathrm{A}}\mathbf{U}(t_n)$;
   - assemble external forces $\mathbf{F}^{ext}(t_n)$;
   - solve for the *master* unknowns $\mathbf{U}_{master}$ the systems (22);
   - perform the projection on the *slave* unknowns;
   - if the final time T is not reached set $t_n \leftarrow t_{n+1}$ and go to 6.

Algorithm 2 describes the DG solution scheme. Here we denote by $\mathbf{J}(t_n) = \underline{\mathrm{B}}\mathbf{U}(t_n)$ the vector containing the interface terms. Since the matrix $\underline{\mathrm{B}}$ defined in (14) has a highly sparsity structure, it is stored taking advantage of it.

Algorithm 2: DG Solution Scheme

1. Set initial conditions $\mathbf{u}_0$ and $\mathbf{u}_1$.
2. Build the skeleton $\mathcal{S}$ for the domain Ω.

3. Decompose $\mathcal{S}$ into elementary components.
4. Construct the matrix $\underline{\mathrm{B}}$ for the interface unknowns.
5. For each discrete time t_n:
   - compute the internal forces $\mathbf{F}^{int}(t_n) = \underline{\mathbf{A}}\mathbf{U}(t_n)$;
   - assemble external forces $\mathbf{F}^{ext}(t_n)$;
   - compute the jumps at the interfaces $\mathbf{J}(t_n) = \underline{\mathrm{B}}\mathbf{U}(t_n)$;
   - solve the system $\underline{\mathbf{M}}\ddot{\mathbf{U}} = \mathbf{F}^{ext}(t_n) - \mathbf{F}^{int}(t_n) - \mathbf{J}(t_n)$;
   - if the final time T is not reached set $t_n \leftarrow t_{n+1}$ and go to 4.

According to [1, 9, 10], it seems that for elastic wave propagation problems the more effective method, in term of accuracy, grid dispersion and stability is the symmetric interior penalty Galerkin method (SIPG). However, if the symmetric approach is used we recall that the constant α in (12) must be sufficiently large to guarantee consistency of the method without affecting the conditioning of the stiffness matrix in (13).

6 A SOIL-STRUCTURE INTERACTION PROBLEM

In this section we aim at studying a soil-structure interaction problem, namely the seismic response of a railway viaduct (Acquasanta viaduct, Genova, Italy). We consider the viscoelastic model (1) in the computational domain $(x, z) \in \Omega = (0, 10^4 m) \times (0, f(x))$, where f describes the top profile of the bridge and of the surrounding valley, see Fig. 3. The size of the domain is chosen in order to avoid any possible interference with reflections of the waves of interest with the spurious ones eventually arising from the absorbing boundaries. The dynamic and mechanical properties of the structure and of the surrounding soil are summarized in Table 6. Depending on the material involved, we subdivided the computational grid into different regions, as shown in Fig. 3 (top panel). Note that the mesh was designed to propagate up to about 3 Hz.

We simulate a point source load of the form $\mathbf{f}(\mathbf{x}, t) = \mathbf{g}(\mathbf{x})h(t)$, where $\mathbf{f}$ is the external force introduced in (1). The function $\mathbf{g}$ describes the space distribution of the source and often is the body force $\mathbf{g}(\mathbf{x}) = \delta(\mathbf{x} - \mathbf{x}_S)\hat{\mathbf{w}}$, where δ represents the Dirac distribution, $\mathbf{x}_S$ is the source location and $\hat{\mathbf{w}}$ is the direction of the body force. The source time history is given by a Ricker-type time function with maximum frequency $\nu_{max} = 3Hz$, defined as

$$h(t) = h_0[1 - 2\beta(t - t_0)^2] \exp[-\beta(t - t_0)^2], \tag{23}$$

where h_0 is a scale factor, $t_0 = 2$ seconds is the time shift and $\beta = \pi^2\nu_{max}^2 = 9.8696\, s^{-1}$ is a parameter that determines the width of the wavelet (23).

In Fig. 3 we show the two different computational grids used for the numerical simulations. The conforming grid, Fig. 3 left, is used with SEM discretization to produce a reference solution for the problem. It provides, in fact, a sufficiently accurate discretization, as we verified that further mesh refinements generates quasi-identical seismograms. The non-conforming grid, shown in Fig. 3 right, is used for both DGSEM and MSEM simulations.

In our analysis we choose the polynomial approximation degree as described in Table 6. It is worth highlighting that the non-conforming approximations lead to a dramatic reduction of the size of the numerical model and, hence, of the computational costs (102.640 unknowns for

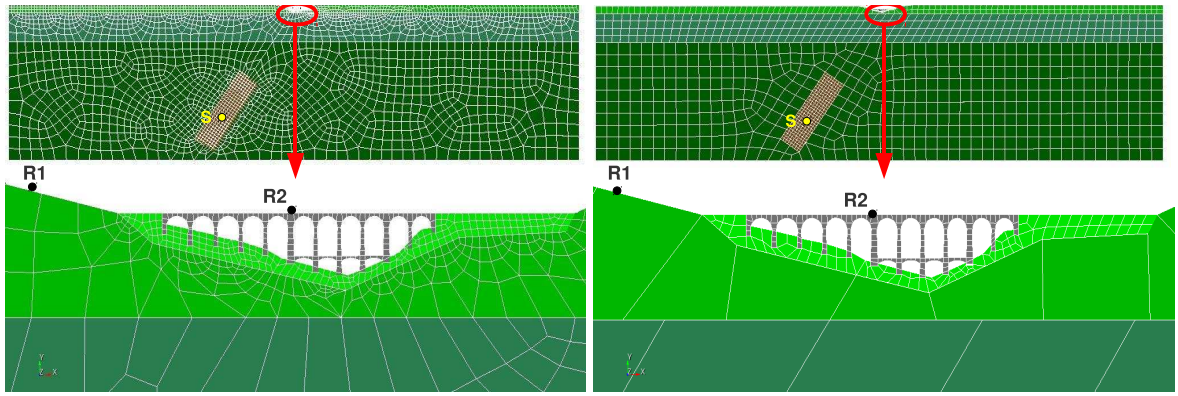

Figure 3: Conforming (left) and non conforming (right) grids. The full domain is displayed on the top and a zoom of the railway bridge is displayed on the bottom. The receivers R1 and R2, on the ground and on the bridge, respectively, are also highlighted.

Layer	$\rho\,[Kg/m^3]$	$c_P\,[m/s]$	$c_S\,[m/s]$	$\zeta[1/s]$	N [SEM]	N [MSEM/DGSEM]
1 (bridge)	1750	1218	716,7	0.6283	4	2
2 (stiff soil)	2400	1100	635	0.31416	4	2
3 (soft bedrock)	2400	1100	635	0.02513	4	4
4 (medium bedrock)	2600	1700	982	0.02284	4	4
5 (stiff bedrock)	2800	2300	1330	0.02094	4	4
6 (stiff bedrock)	2800	2300	1330	0.02094	4	4

Table 1: Dynamic and mechanical parameters and polynomial approximation degree N for each subregion of the domain decomposition (the factor ζ takes into account the visco-elastic linear soil behavior).

SEM vs. 41.322 for MSEM or DGSEM).
Such an advantage is expected to play a major role for 3D engineering applications. In Fig. 4 (resp Fig. 5 we analyse the synthetic seismograms recorded by the receiver R1 (resp. R2) on the top of the ground (resp. bridge) using the misfits criteria introduced in [19]. The results shown an excellent fit of the data for R1 and a good fit for R2. Probably, for the latter receiver, the results are affected by the grid dispersion phenomenon arising when low order polynomial approximation degrees are used [1, 9, 10].

7 CONCLUSIONS

In this paper we compared two different non-conforming high order numerical techniques, namely the Mortar Spectral Element Method and the Discontinuous Galerkin Spectral Element Method, for the approximation of the elastic wave equation in heterogeneous media. The key feature of these methods is to replace the exact continuity condition at the skeleton of the decomposition with a weak one, written in terms of the jumps of the displacements and the tractions across the interfaces. Relaxing the continuity condition is then possible, preserving the accuracy of high order methods, to deal with a geometrically non-conforming domain partitions where local meshes are independently generated from the neighbouring ones and associated with different spectral approximation degrees. Note that the subdomain partition is constructed according to the (available) material properties. Starting from a common weak formulation we describe both approaches in parallel in order to highlight their analogies and their differences. We gave a special attention to the implementation aspects of the two techniques in order to make the reader able to deal with an efficient numerical coding. Finally, we show that the MSEM and the DGSEM can be effectively used for complex seismic wave propagation problems, namely the soil-structure interaction between a valley and a railway bridge. The results, compared with those obtained with the SEM, show that both the non-conforming strategies are good in term of accuracy and computational effort. We refer to [1] for the full comparison of the methods in term of convergence, accuracy, grid dispersion and stability.

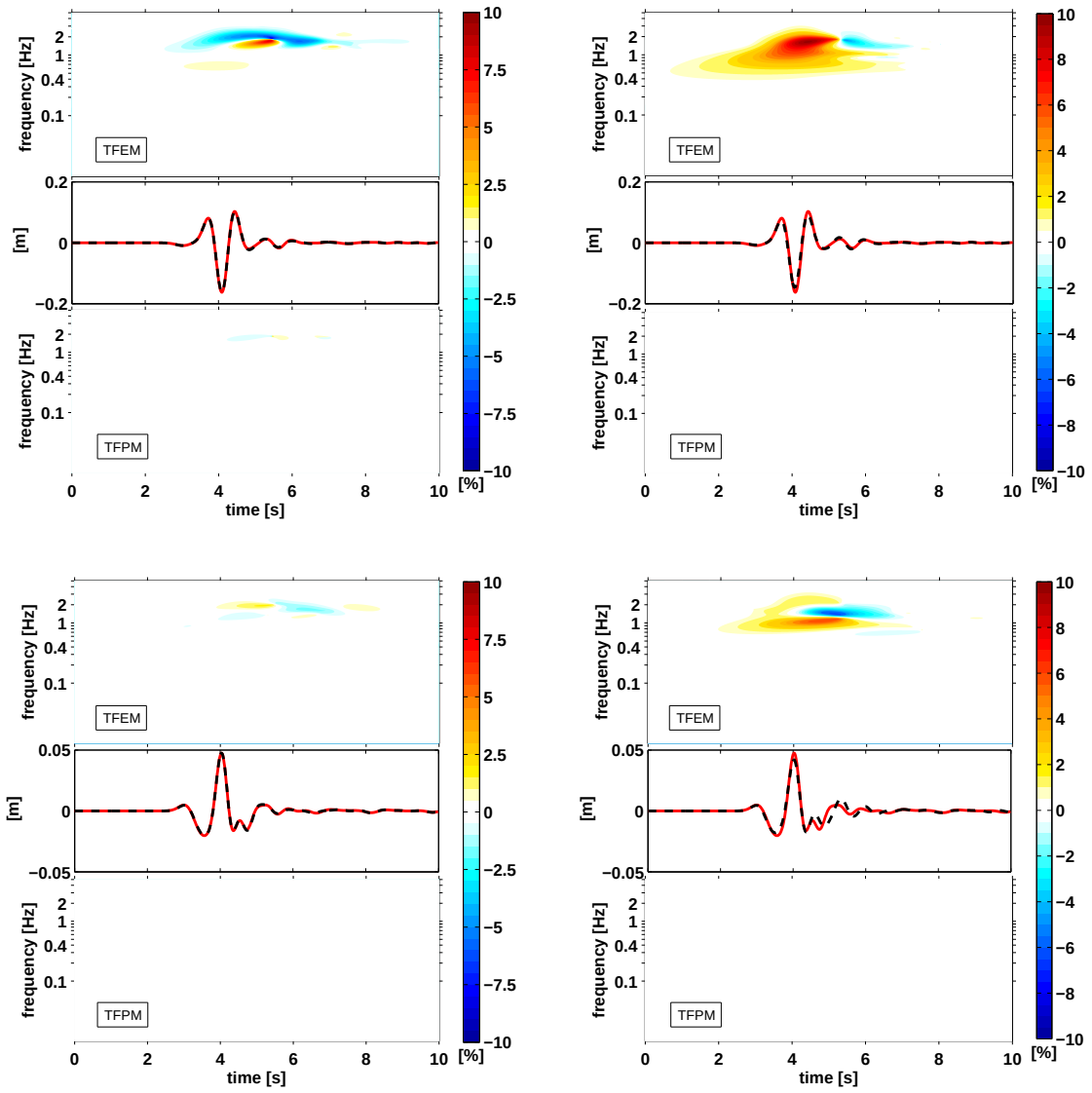

Figure 4: Analysis of the synthetic signals recorded by receiver R1, using the misfits criteria described in [19]. Comparison between the synthetic seismograms obtain with SEM and DGSEM (left) and SEM and MSEM (right). The graphics are subdivided as follows. Middle: displacement obtained using conforming (solid line) and non conforming (dashed line) approximations. TFEM: time frequency envelope misfits. TFPM: time frequency phase misfits. Top: horizontal component. Bottom: vertical component.

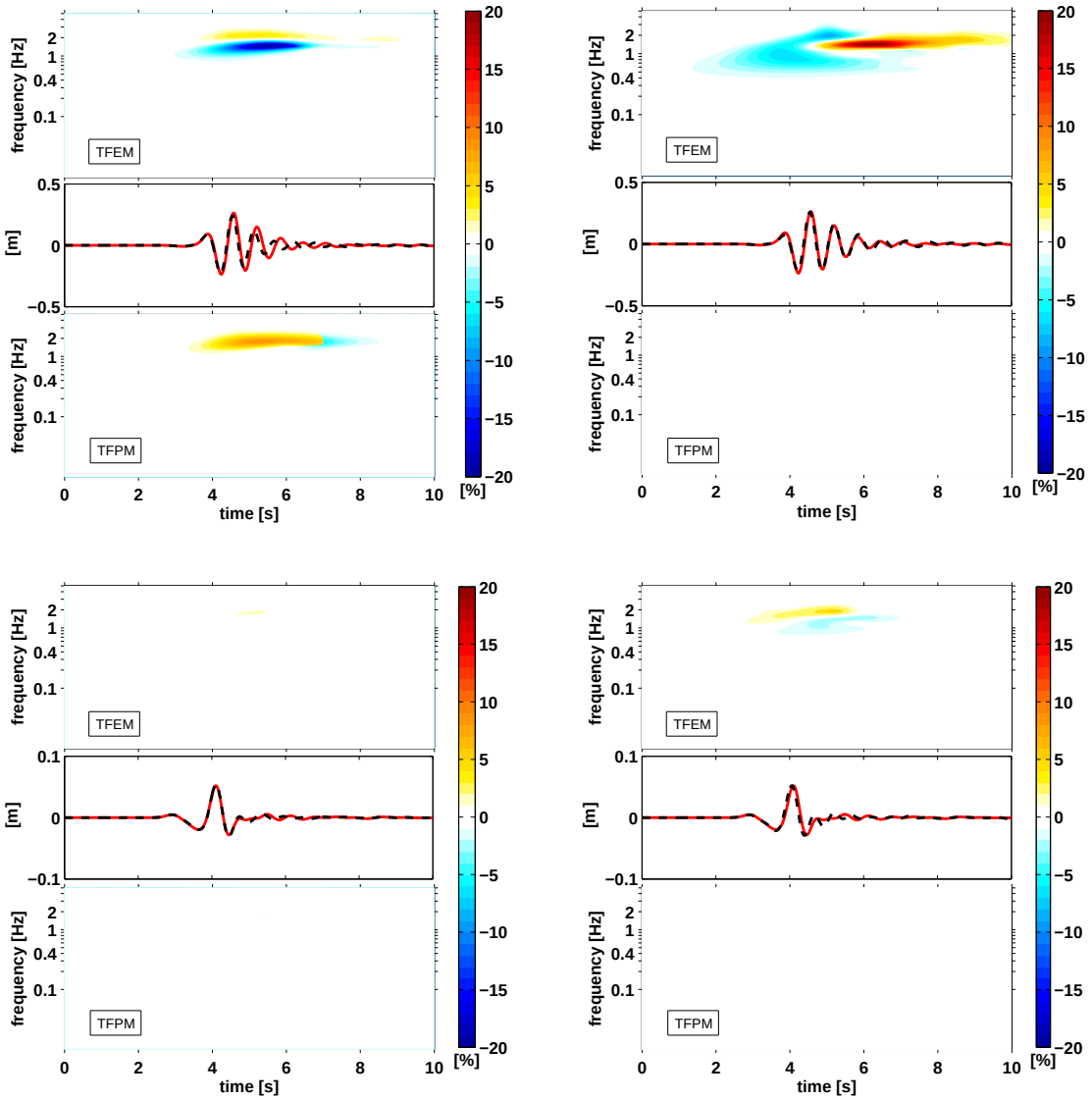

Figure 5: As in Fig. 4 but for receiver R2.

REFERENCES

[1] P. F. Antonietti, I. Mazzieri, A. Quarteroni, and F. Rapetti. In preparation.

[2] D. N. Arnold, F. Brezzi, B. Cockburn, and L. D. Marini. Unified analysis of discontinuous Galerkin methods for elliptic problems. *SIAM J. Numer. Anal.*, 39(5):1749–1779 (electronic), 2001/02.

[3] C. Bernardi, Y. Maday, and A. T. Patera. A new nonconforming approach to domain decomposition: the mortar element method. In *Nonlinear partial differential equations and their applications. Collège de France Seminar, Vol. XI (Paris, 1989–1991)*, volume 299 of *Pitman Res. Notes Math. Ser.*, pages 13–51. Longman Sci. Tech., Harlow, 1994.

[4] S. C. Brenner and L. R. Scott. *The mathematical theory of finite element methods*, volume 15 of *Texts in Applied Mathematics*. Springer, New York, third edition, 2008.

[5] E. Chaljub, Y. Capdeville, and J.P. Vilotte. Solving elastodynamics in a fluid-solid heterogeneous sphere: a parallel spectral element approximation on non-conforming grids. *J. Comput. Phys.*, 187(2): 457–491, 2003

[6] C. Canuto, M. Y. Hussaini, A. Quarteroni, and T. A. Zang. *Spectral methods*. Scientific Computation. Springer-Verlag, Berlin, 2006. Fundamentals in single domains.

[7] C. Canuto, M. Y. Hussaini, A. Quarteroni, and T. A. Zang. *Spectral methods*. Scientific Computation. Springer, Berlin, 2007. Evolution to complex geometries and applications to fluid dynamics.

[8] F. Casadei, E. Gabellini, G. Fotia, F. Maggio, and A. Quarteroni. A mortar spectral/finite element method for complex 2D and 3D elastodynamic problems. *Comput. Methods Appl. Mech. Engrg.*, 191(45):5119–5148, 2002.

[9] J. D. De Basabe and M. K. Sen. Stability of the high-order finite elements for acoustic or elastic wave propagation with high-order time stepping. *Geophys. J. Int.*, 181(1):577–590, 2010.

[10] J. D. De Basabe, M. K. Sen, and M. F. Wheeler. The interior penalty discontinuous galerkin method for elastic wave propagation: grid dispersion. *Geophys. J. Int.*, 175(1):83–93, 2008.

[11] M. O. Deville, P. F. Fisher, and E. H. Mund. *High-Order Methods for Incompressible Fluid Flow*. Cambridge Monographs on Applied and Computational Mathematics. Cambridge University Press, The Edinburgh Building, Cambridge CB2 2RU, UK, 2002.

[12] E. Faccioli, F. Maggio, R. Paolucci, and A. Quarteroni. 2-D and 3-D elastic wave propagation by a pseudo-spectral domain decomposition method. *J. of Seismol.*, 1: 237–251, 1997.

[13] M.J. Grote, A. Schneebeli, and D. Schotzau. Discontinuous Galerkin finite element method for the wave equation. *SIAM J. Numer. Anal.*, 44(6): 2408–2431, 2006.

[14] Numerical code GeoELSE: http://geoelse.stru.polimi.it

[15] J. de la Puente, M. Käser, M. Dumbser, and H. Igel. An arbitrary high-order discontinuous Galerkin method for elastic waves on unstructured meshes – IV. Anisotropy. *Geophys. J. Int.*, 169(3): 1210–1228, 2007.

[16] D. Komatitsch and J. Tromp. Introduction to the spectral-element method for 3-D seismic wave propagation. *Geophys. J. Int.*, 139: 806–822, 1999.

[17] G. Seriani, E. Priolo, J. Carcione, and E. Padovani. High-order spectral element method for elastic wave modeling. In *Expanded abstracts of the SEG, 62nd Int. Mtng of the SEG*, New Orleans.

[18] R. Kosloff, and D. Kosloff. Absorbing boundaries for wave propagation problems. *J. Comput. Phys.*, 63(2): 363–376, 1986.

[19] M. Kristeková, J. Kristek, and P. Moczo. Time-frequency misfit and goodness-of-fit criteria for quantitative comparison of time signals. *Geophys. J. Int.*, 178: 813–825, 2009.

[20] E.D. Mercerat, J.P. Vilotte, and F.J. Sánchez-Sesma. Triangular Spectral Element simulation of two-dimensional elastic wave propagation using unstructured triangular grids. *Geophys. J. Int*, 166: 679–698, 2006.

[21] Y. Maday, C. Mavriplis, and A. T. Patera. Nonconforming mortar element methods: application to spectral discretizations. In *Domain decomposition methods (Los Angeles, CA, 1988)*, pages 392–418. SIAM, Philadelphia, PA, 1989.

[22] A. Quarteroni and A. Valli. *Numerical approximation of partial differential equations*, volume 23 of *Springer Series in Computational Mathematics*. Springer-Verlag, Berlin, 1994.

[23] P.-A. Raviart and J.-M. Thomas. *Introduction à l'analyse numérique des équations aux dérivées partielles*. Collection Mathématiques Appliquées pour la Maîtrise. [Collection of Applied Mathematics for the Master's Degree]. Masson, Paris, 1983.

[24] B. Rivière. *Discontinuous Galerkin methods for solving elliptic and parabolic equations*, volume 35 of *Frontiers in Applied Mathematics*. Society for Industrial and Applied Mathematics (SIAM), Philadelphia, PA, 2008. Theory and implementation.

[25] B. Rivière, S. Shaw, M. F. Wheeler, and J. R. Whiteman. Discontinuous Galerkin finite element methods for linear elasticity and quasistatic linear viscoelasticity. *Numer. Math.*, 95(2):347–376, 2003.

[26] B. Rivière and M. F. Wheeler. Discontinuous finite element methods for acoustic and elastic wave problems. In *Current trends in scientific computing (Xi'an, 2002)*, volume 329 of *Contemp. Math.*, pages 271–282. Amer. Math. Soc., Providence, RI, 2003.

[27] R. Stacey. Improved transparent boundary formulations for the elastic-wave equation. *Bullettin of the Seismological Society of America*, 78(6):2089–2097, 1988.